

# Glass forming ability and magnetic properties of $\text{Nd}_{48}\text{Al}_{20}\text{Fe}_{27}\text{Co}_5$ bulk metallic glass with distinct glass transition

L Xia<sup>1,2,3</sup>, M B Tang<sup>2</sup>, M X Pan<sup>2</sup>, W H Wang<sup>2</sup> and Y D Dong<sup>1</sup>

<sup>1</sup> Institute of Materials, Shanghai University, Shanghai 200072, People's Republic of China

<sup>2</sup> Institute of Physics, Chinese Academy of Science, Beijing 100080, People's Republic of China

E-mail: xialei@mail.shu.edu.cn

Received 5 January 2004

Published 26 May 2004

Online at [stacks.iop.org/JPhysD/37/1706](http://stacks.iop.org/JPhysD/37/1706)

DOI: 10.1088/0022-3727/37/12/017

## Abstract

$\text{Nd}_{48}\text{Al}_{20}\text{Fe}_{27}\text{Co}_5$  bulk metallic glass (BMG) was prepared in the shape of rods 3 mm in diameter by suction casting. In contrast to the previously reported hard magnetic Nd–Al–Fe–Co BMGs, the  $\text{Nd}_{48}\text{Al}_{20}\text{Fe}_{27}\text{Co}_5$  as-cast rod exhibits a distinct glass transition, multi-step crystallizations in DSC traces and much lower coercivity. The glass forming ability as well as the kinetics of the glass transition and crystallizations of the  $\text{Nd}_{48}\text{Al}_{20}\text{Fe}_{27}\text{Co}_5$  as-cast rod have been studied. The magnetic properties of the alloy were investigated in comparison with  $\text{Nd}_{60}\text{Al}_{10}\text{Fe}_{20}\text{Co}_{10}$  glass forming alloys.

## 1. Introductions

In recent years, rare-earth–transition-metal (RE–TM) metallic glasses with promising magnetic properties and excellent glass forming ability have attracted increasing interest because of their great significance in materials science and their considerable technological promise [1–5]. The magnetic amorphous alloys studied include Nd(Pr)–Fe(Co)–Al [3–10], Nd–Fe–Co–Al–B [11], Nd(Pr)–Al–Ni–Cu–Fe(Co) [2], Y–Fe–Al [12], and so on. Among these, Nd–Fe(Co)–Al bulk metallic glasses (BMGs) have shown attractive glass-forming ability (GFA), high coercivity and absence of glass transition in DSC traces [3–10]. Inoue *et al* [4] supposed that the high coercivity of the alloys is due to the pre-existence of ferromagnetic clusters, the glass transition temperature being higher than the crystallization temperature, and the reduced glass transition temperature was estimated to be higher than 0.9. Recent experimental results have shown that the BMGs are partially crystalline [13] and the absence of glass transition in DSC traces might be due to the chemical inhomogeneity of the amorphous phase [14]. More recently, further results obtained in  $\text{Nd}_{60}\text{Al}_{10}\text{Fe}_{20}\text{Co}_{10}$  glass-forming alloys have revealed that the typical microstructure of nano-scale particles scattering in the amorphous matrix is closely related to

the primary crystallization (observed in the DSC traces of the ribbons) of the alloy [13, 15] and the reduced glass transition temperature representing the GFA might not match the value reported previously [14, 15]. Up to now, the glass transition of the bulk samples could only be obtained in the DSC traces of the paramagnetic  $\text{Nd}_{60}\text{Co}_{30}\text{Al}_{10}$  amorphous rods [5] and the partially crystalline  $\text{Nd}_{60}\text{Al}_{10}\text{Co}_{30-x}\text{Fe}_x$  ( $x < 10$ ) rods [16], and it is generally regarded that both the hard magnetic properties and the absence of glass transition were related to the existence of partially crystalline Nd–Fe-rich clusters [4, 13, 14].

In this work, we report the formation of  $\text{Nd}_{48}\text{Al}_{20}\text{Fe}_{27}\text{Co}_5$  BMG with distinct glass transition and much softer magnetic properties. The glass forming ability and the kinetic characters of the BMG were studied. The magnetic properties of the BMG were investigated in comparison with  $\text{Nd}_{60}\text{Al}_{10}\text{Fe}_{20}\text{Co}_{10}$  as-cast rods.

## 2. Experiments

Ingots with nominal compositions of  $\text{Nd}_{48}\text{Al}_{20}\text{Fe}_{27}\text{Co}_5$  and  $\text{Nd}_{60}\text{Al}_{10}\text{Fe}_{20}\text{Co}_{10}$  were prepared by arc-melting of 99.9% (at.%) pure Nd, Fe, Al and Co in a titanium-gettered Ar atmosphere.  $\text{Nd}_{48}\text{Al}_{20}\text{Fe}_{27}\text{Co}_5$  and  $\text{Nd}_{60}\text{Al}_{10}\text{Fe}_{20}\text{Co}_{10}$  cylinders 3 mm in diameter were prepared by suction casting

<sup>3</sup> Author to whom any correspondence should be addressed.

under an argon atmosphere. The as-cast rod samples investigated in this work were taken from the central region of the cylinders and the element distribution of the sample was detected to be homogeneous within the detection limit of a HITACHI S-570 energy dispersive spectrometer (EDS). The structure of the samples was characterized by XRD in a Philips diffractometer using  $\text{Cu } K_\alpha$  radiation. A vibrating sample magnetometer (VSM) was used for the magnetic measurements of the as-cast rods. The field applied was  $1432 \text{ kA m}^{-1}$ . DSC measurements were carried out under a purified argon atmosphere in a Perkin Elmer DSC-7 at heating rates ranging from 10 to  $80 \text{ K min}^{-1}$ . The calorimeter was calibrated for temperature and energy at various heating rates with high purity indium and zinc. An empty Al pan was first scanned to establish a baseline, and then the same Al pan with the sample was scanned again under identical thermal conditions.

### 3. Results and discussions

Figure 1 shows the XRD patterns of  $\text{Nd}_{48}\text{Al}_{20}\text{Fe}_{27}\text{Co}_5$  and  $\text{Nd}_{60}\text{Al}_{10}\text{Fe}_{20}\text{Co}_{10}$  as-cast rods. The typical broad diffraction maxima in XRD patterns show the fully amorphous characters of  $\text{Nd}_{48}\text{Al}_{20}\text{Fe}_{27}\text{Co}_5$  and  $\text{Nd}_{60}\text{Al}_{10}\text{Fe}_{20}\text{Co}_{10}$  as-cast rods within the XRD detection limit. No obvious crystalline peaks were found.

The continuous DSC traces obtained from  $\text{Nd}_{48}\text{Al}_{20}\text{Fe}_{27}\text{Co}_5$  and  $\text{Nd}_{60}\text{Al}_{10}\text{Fe}_{20}\text{Co}_{10}$  as-cast rods at a heating rate of  $20 \text{ K min}^{-1}$  are shown in figure 2. There is no glass transition in the DSC trace of the  $\text{Nd}_{60}\text{Al}_{10}\text{Fe}_{20}\text{Co}_{10}$  as-cast rod and the crystallization behaviour is complicated [17]. In contrast,  $\text{Nd}_{48}\text{Al}_{20}\text{Fe}_{27}\text{Co}_5$  as-cast rods exhibit the endothermic characteristics of a glass transition followed by three exothermic crystallization peaks and a sharp endothermic melting peak. The primary crystallization can also be found in the DSC traces of amorphous  $\text{Nd}_{57}\text{Al}_{10}\text{Fe}_{20}\text{Co}_5\text{B}_8$  [11],  $\text{Nd}_{60}\text{Fe}_{30}\text{Al}_{10}$  ( $30 \text{ m s}^{-1}$ ) [18], and  $\text{Nd}_{60}\text{Al}_{10}\text{Fe}_{20}\text{Co}_{10}$  [13] as-spun ribbons but it is invisible in the DSC traces of their bulk counterparts. The onset temperatures of the glass transition ( $T_g$ ), melting ( $T_m$ ) and crystallizations ( $T_{x1}$ ,  $T_{x2}$  and  $T_{x3}$ ) obtained from the DSC trace of  $\text{Nd}_{48}\text{Al}_{20}\text{Fe}_{27}\text{Co}_5$  as-cast rods are observed to be about 495, 798, 537, 697 and 742 K. The liquidus temperature of the alloy is about 834 K. Thus, the

supercooled liquid region ( $\Delta T = T_x - T_g$ ) and the reduced glass transition temperature ( $T_{rg} = T_g/T_l$ ) of the alloy are about 42 K and 0.594 K, respectively. The alloy exhibits a relatively large GFA. Lu and Liu have recently studied the GFA for various glass forming systems from devitrification and amorphization perspectives, and have found that the GFA for non-crystalline materials was related mainly to  $1/(T_g + T_l)$  and  $T_x$ . They, therefore, defined a new parameter  $\gamma = T_x/(T_g + T_l)$  for predicting the GFA of alloys [19, 20]. The parameter has been confirmed to be valid in various glass forming systems. Concerning the GFA of the  $\text{Nd}_{48}\text{Al}_{20}\text{Fe}_{27}\text{Co}_5$  alloy, the value of  $\gamma$  for the alloy can be calculated to be 0.404. Hence, the critical cooling rate  $R_c$  can also be obtained from the linear relationship between  $\gamma$  values and  $\log_{10} R_c$  expressed as  $R_c = C_1 \exp(-117.19\gamma)$ , where  $C_1$  is a constant, which for metallic glass is  $5.1 \times 10^{21} \text{ K s}^{-1}$  [19].  $R_c$  of the alloy is estimated to be  $10.9 \text{ K s}^{-1}$ . The critical section thickness ( $Z_c = 2.80 \times 10^{-7} \exp(41.70\gamma)$ ) [19] can also be predicted to be 5.8 mm. They are roughly in accordance with our recent experimental results and, thus, the parameter  $\gamma$  is reliable for the prediction of the GFA of  $\text{Nd}_{48}\text{Al}_{20}\text{Fe}_{27}\text{Co}_5$  BMG.

To investigate the glass transition and crystallization behaviour in more detail, DSC measurements of  $\text{Nd}_{48}\text{Al}_{20}\text{Fe}_{27}\text{Co}_5$  as-cast rods were carried out at heating rates ( $\phi$ ) of 10, 20, 40 and  $80 \text{ K min}^{-1}$  (as shown in figures 3(a) and (b)). The glass transition temperature and crystallization temperatures shift to higher values with increasing heating rates indicating a marked kinetic character. The kinetics of the glass transition and crystallizations can be analysed using the Kissinger equation:  $\ln(T^2/\phi) = \ln(E/(k_B K_0)) + E/(k_B T)$ , where  $k_B$  is the Boltzman constant,  $E$  is the effective activation energy and  $K_0$  is the frequency factor in the Arrhenius Law [21]. Figure 3(c) shows the Kissinger plots and their linear fittings for the onset temperature of the glass transition and the peak temperatures of crystallizations. The effective activation energies for glass transition ( $E_g$ ), primary crystallization ( $E_{x1}$ ), second crystallization ( $E_{x2}$ ) and third crystallization ( $E_{x3}$ ) were determined by fitting the Kissinger equation to the experimental data plots. Their values are 2.9 eV, 1.8 eV, 1.7 eV and 1.9 eV, respectively.

The hysteresis loops of the  $\text{Nd}_{48}\text{Al}_{20}\text{Fe}_{27}\text{Co}_5$  and  $\text{Nd}_{60}\text{Al}_{10}\text{Fe}_{20}\text{Co}_{10}$  as-cast rods are shown in figure 4. The magnetization ( $M$ ) at  $1432 \text{ kA m}^{-1}$  of the  $\text{Nd}_{48}\text{Al}_{20}\text{Fe}_{27}\text{Co}_5$

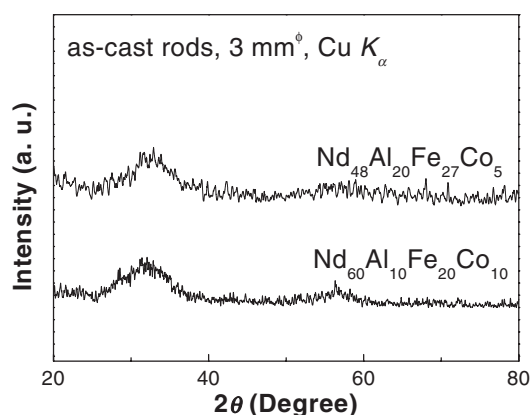


Figure 1. XRD patterns of  $\text{Nd}_{48}\text{Al}_{20}\text{Fe}_{27}\text{Co}_5$  and  $\text{Nd}_{60}\text{Al}_{10}\text{Fe}_{20}\text{Co}_{10}$  as-cast rods.

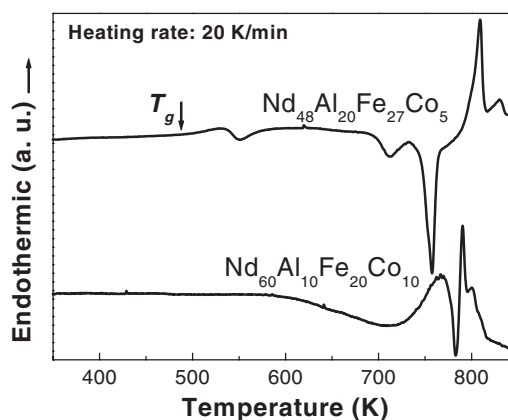
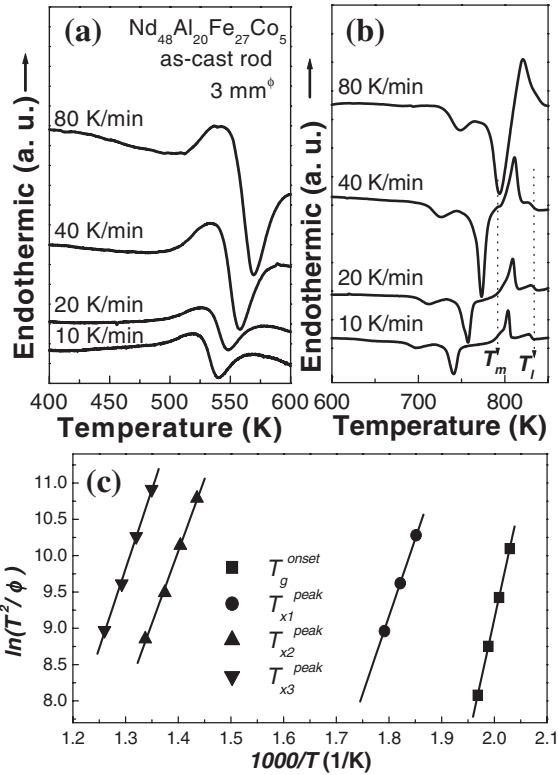
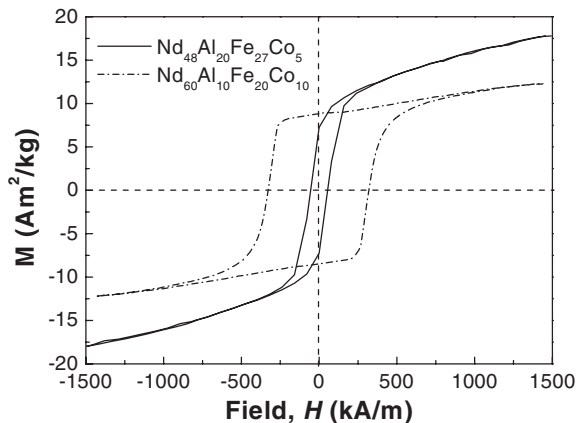


Figure 2. DSC traces of  $\text{Nd}_{48}\text{Al}_{20}\text{Fe}_{27}\text{Co}_5$  and  $\text{Nd}_{60}\text{Al}_{10}\text{Fe}_{20}\text{Co}_{10}$  as-cast rods at a heating rate of  $20 \text{ K min}^{-1}$ .



**Figure 3.** DSC traces of the  $\text{Nd}_{48}\text{Al}_{20}\text{Fe}_{27}\text{Co}_5$  as-cast rod at a heating rate of 10, 20, 40 and 80  $\text{K min}^{-1}$  from (a) 400 to 600 K and (b) 600 to 850 K. (c) shows the Kissinger plots and their linear fitting of glass transition and crystallizations.



**Figure 4.** Hysteresis loops of  $\text{Nd}_{48}\text{Al}_{20}\text{Fe}_{27}\text{Co}_5$  and  $\text{Nd}_{60}\text{Al}_{10}\text{Fe}_{20}\text{Co}_{10}$  as-cast rods.

as-cast sample is  $17.8 \text{ Am}^2 \text{ kg}^{-1}$  (higher than the magnetization of the  $\text{Nd}_{60}\text{Al}_{10}\text{Fe}_{20}\text{Co}_{10}$  as-cast rod) while the coercivity ( $H_c$ ) is  $50 \text{ kA m}^{-1}$ . The higher value of magnetization of the  $\text{Nd}_{48}\text{Al}_{20}\text{Fe}_{27}\text{Co}_5$  as-cast sample could be due to the increase in the content of Fe. It should be noticed that the coercivity of the  $\text{Nd}_{48}\text{Al}_{20}\text{Fe}_{27}\text{Co}_5$  bulk sample is much lower than that of the  $\text{Nd}_{60}\text{Al}_{10}\text{Fe}_{20}\text{Co}_{10}$  as-cast rod (about  $330 \text{ kA m}^{-1}$ ) and almost equals that of the  $\text{Nd}_{60}\text{Al}_{10}\text{Fe}_{20}\text{Co}_{10}$  as-spun ribbons obtained at a higher cooling rate (about  $30\text{--}70 \text{ kA m}^{-1}$ ) [13]. Previous studies have revealed that the coercivity of the bulk  $\text{Nd}_{60}\text{Al}_{10}\text{Fe}_{20}\text{Co}_{10}$  and  $\text{Nd}_{60}\text{Al}_{10}\text{Fe}_{30}$  samples is closely related to the *in situ* formation of partially

crystalline hard magnetic nano-particles in the amorphous matrix, while the fully amorphous ribbons exhibit nearly soft magnetic properties [6, 13, 15]. Therefore, the nearly soft magnetic  $\text{Nd}_{48}\text{Al}_{20}\text{Fe}_{27}\text{Co}_5$  as-cast sample could be amorphous and contains few clusters. On the other hand, concerning the glass forming ability of the alloys, the reduced glass transition temperature of  $\text{Nd}_{48}\text{Al}_{20}\text{Fe}_{27}\text{Co}_5$  is much higher than that of  $\text{Nd}_{60}\text{Al}_{10}\text{Fe}_{20}\text{Co}_{10}$  alloys ( $<0.52$ ) [15]. It is known that the nucleation rate in glass forming alloys is controlled by the cooling rate and the intrinsic GFA (normally represented by  $T_{\text{rg}}$ ) of the alloys [22]. At the same cooling rate, the higher  $T_{\text{rg}}$  is, the lower is the nucleation rate. The nucleation rate of the hard magnetic phases and the amount of these particles in the  $\text{Nd}_{48}\text{Al}_{20}\text{Fe}_{27}\text{Co}_5$  as-cast rod with higher  $T_{\text{rg}}$  could be much lower than those in the  $\text{Nd}_{60}\text{Al}_{10}\text{Fe}_{20}\text{Co}_{10}$  as-cast rod. Thus, the coercivity dominated by the volume fraction of hard magnetic particles [23–25] could be lower in the  $\text{Nd}_{48}\text{Al}_{20}\text{Fe}_{27}\text{Co}_5$  as-cast rod than in the  $\text{Nd}_{60}\text{Al}_{10}\text{Fe}_{20}\text{Co}_{10}$  as-cast rod.

#### 4. Conclusions

In conclusion, the glass forming ability, kinetic characters and magnetic properties of  $\text{Nd}_{48}\text{Al}_{20}\text{Fe}_{27}\text{Co}_5$  BMG were investigated in comparison with that of the  $\text{Nd}_{60}\text{Al}_{10}\text{Fe}_{20}\text{Co}_{10}$  glass forming alloy. In contrast to  $\text{Nd}_{60}\text{Al}_{10}\text{Fe}_{20}\text{Co}_{10}$  bulk as-cast samples, the  $\text{Nd}_{48}\text{Al}_{20}\text{Fe}_{27}\text{Co}_5$  as-cast rod exhibits a distinct glass transition in DSC traces and much softer magnetic properties. The obtained values of  $T_{\text{rg}} (=0.594)$  and the parameter  $\gamma (=0.404)$  of the  $\text{Nd}_{48}\text{Al}_{20}\text{Fe}_{27}\text{Co}_5$  as-cast rod indicate the excellent glass forming ability of the alloy. The critical cooling rate and section thickness of the BMG were estimated to be  $10.9 \text{ K s}^{-1}$  and 5.8 mm. The kinetics of glass transition and crystallizations of the  $\text{Nd}_{48}\text{Al}_{20}\text{Fe}_{27}\text{Co}_5$  alloy were analysed by the Kissinger method and the effective activation energies ( $E_g$ ,  $E_{x1}$ ,  $E_{x2}$  and  $E_{x3}$ ) were obtained to be 2.9, 1.8, 1.7 and 1.9 eV. The magnetization and coercivity of the  $\text{Nd}_{48}\text{Al}_{20}\text{Fe}_{27}\text{Co}_5$  as-cast rod were measured to be  $17.8 \text{ Am}^2 \text{ kg}^{-1}$  and  $50 \text{ kA m}^{-1}$ . The relationship between hard magnetic properties and the glass forming ability was discussed, and low coercivity in  $\text{Nd}_{48}\text{Al}_{20}\text{Fe}_{27}\text{Co}_5$  BMG is supposed to be related to the high GFA of the alloy.

#### Acknowledgments

The authors are thankful for the financial support of the National Nature Science Foundation of China (Grant Nos 59925101, 50031010 and 10174088).

#### References

- [1] Croat J J 1982 *J. Appl. Phys.* **53** 3161
- [2] He Y, Price C E, Poon S J and Shiflet G J 1994 *Phil. Mag. Lett.* **70** 371
- [3] Inoue A, Zhang T, Zhang W and Takeuchi A 1996 *Mater. Trans. JIM* **37** 99
- [4] Inoue A, Takeuchi A and Zhang T 1998 *Metall. Mater. Trans. A* **29** 1779
- [5] Inoue A and Zhang T 1997 *Mater. Sci. Eng. A* **226–228** 393
- [6] Schneider S, Bracchi A, Samwer K, Seibt M and Thiyagarajan P 2002 *Appl. Phys. Lett.* **80** 1749
- [7] Ding J, Li Y and Wang X Z 1999 *J. Phys. D: Appl. Phys.* **32** 713

- [8] Fan G J, Löser W, Roth S, Eckert J and Schultz L 2000 *J. Mater. Res.* **15** 1556
- [9] Wei B C, Zhang Y, Zhuang Y X, Zhao D Q, Pan M X, Wang W H and Hu W R 2001 *J. Appl. Phys.* **89** 3529
- [10] Wei B C, Wang W H, Pan M X, Han B S and Zhang Z R 2001 *Phys. Rev. B* **64** 012406
- [11] Xing L Q, Eckert J, Löser W, Roth S and Schultz L 2000 *J. Appl. Phys.* **88** 3565
- [12] Wang L, Ding J, Li Y, Kong H Z, Feng Y P and Wang X Z 2000 *J. Phys.: Condens. Matter* **12** 4253
- [13] Xia L, Wei B C, Zhang Z, Pan M X, Wang W H and Dong Y D 2003 *J. Phys. D: Appl. Phys.* **36** 775
- [14] Wei B C, Löser W, Xia L, Roth S, Pan M X, Wang W H and Eckert J 2002 *Acta Mater.* **50** 4357
- [15] Xia L, Tang M B, Wei B C, Pan M X, Zhao D Q, Wang W H and Dong Y D 2003 *J. Phys. D: Appl. Phys.* **36** 2954
- [16] Kumar G, Eckert J, Roth S, Löser W, Schultz L and Ram S 2003 *Acta Mater.* **51** 229
- [17] Xia L, Wei B C, Pan M X, Zhao D Q, Wang W H and Dong Y D 2003 *J. Phys.: Condens. Matter* **15** 3531
- [18] Wang X Z, Li Y, Ding J, Si L and Kong H Z 1999 *J. Alloys Compounds* **290** 209
- [19] Lu Z P and Liu C T 2002 *Acta Mater.* **50** 3501
- [20] Lu Z P and Liu C T 2003 *Phys. Rev. Lett.* **91** 115505-1
- [21] Kissinger H E 1956 *J. Res. Natl Bur. Stand.* **57** 217
- [22] Turnbull D 1969 *Contemp. Phys.* **10** 473
- [23] Randrianantoandro N, Slawska-Waniewska A and Greneche J M 1997 *Phys. Rev. B* **56** 10979
- [24] Arcas J, Hernando A, Barandiarán J M, Prados C, Vázquez M and Marín P 1998 *Phys. Rev. B* **58** 5193
- [25] Löffler J F, Braun H B and Wagner W 2000 *Phys. Rev. Lett.* **85** 1990